

## Influence of graphite morphology, thermal history and S and Cu on ferrite/pearlite formation in cast iron

Hideo Nakae<sup>1</sup>, Ying Zou<sup>2</sup> and Yuya Sato<sup>3</sup>

<sup>1</sup> Professor emeritus, Waseda Univ., Tokyo, Japan

<sup>2</sup> PhD. Student, Waseda Univ., Present address: Nanjing Tech University, Nanjing, China

<sup>3</sup> Student, Waseda Univ., Present address: Cyber Agent, Inc., Tokyo, Japan

**Abstract:** Ferrite and pearlite formation in cast iron is a more complicated phenomenon than that in steel. For example, we cannot observe any ferrite in hyper eutectoid steel, nevertheless, we often observe ferrite in cast iron in spite of its hyper eutectoid composition due to the silicon content. The eutectoid transformation in cast iron was then investigated using as-cast and heat-treated samples. The heating temperature of the cast iron determines the solubility of carbon in the austenite and the content significantly affects the eutectoid transformation. This is the main reason for the fully pearlite matrix in as-cast flake graphite cast iron samples. These results were analyzed and verified by a cooling curves analysis.

For discussing the difference in the matrix structure between the flake and spheroidal graphite cast iron, the influence of sulfur and copper was investigated using high purity flake graphite irons. The results show that sulfur is a very potent pearlite forming element; if the sulfur content is less than 0.0025%, ferrite is the major structure and for more than 0.01%S, the matrix is pearlite, but the copper did not affect the matrix structure of the flake graphite cast iron. This is the main reason why the bull's eye structure is so popular in spheroidal cast iron.

**Keywords:** *eutectoid transformation, ferrite, pearlite, sulfur, copper, flake graphite, spheroidal graphite, diffusion of carbon*

### 1. Introduction

The mechanical properties of cast iron can be controlled by the graphite morphology and matrix, especially, in spheroidal graphite cast iron, the matrix significantly affects them. A small number of papers have described the pearlite and ferrite formation mechanism in cast iron [1-3]. There is a significant difference in the ferrite formation between steel and cast iron. We cannot usually observe the ferrite in hyper eutectoid steel, nevertheless, we often observe ferrite in cast iron in spite of its hyper eutectoid composition due to its silicon content. The objective of the study described in this paper was the specific determination of the

mechanism which controls the matrix structure in the flake and spheroidal graphite cast irons.

As is well known, the matrix of the as-cast flake graphite cast iron is mainly pearlite, nevertheless, that of the spheroidal graphite cast iron consists of ferrite and pearlite, called the bull's eye structure. After heat treatment, such as normalizing, the matrix of the flake graphite cast iron consists of a small amount of ferrite and also graphite; however, the spheroidal one is fully pearlite. Why? We called these phenomena due to the influence of the thermal history and graphite morphology.

If we consider the austenitization temperature during heat treatment for cast iron, the carbon content in the austenite is a function of the heating temperature due to the solubility of carbon in the austenite [4-6]. We then have to study the influence of the heating temperature on the matrix of the flake graphite cast iron.

We also considered that the significant difference in the effect of the alloying element between the flake and spheroidal graphite cast irons should be the activity of sulfur [6], then we discussed the influence of sulfur on the matrix of the flake graphite cast iron using high purity materials for making significantly low sulfur iron. Comparing the matrix structure with the spheroidal one, we discuss the effect of sulfur on the pearlite formation in the cast iron.

### 2. Experimental procedure

In this study, we carried out two experiments, i.e., experiment-1 and experiment-2. In experiment-1, the object was the specific investigation of the difference in the matrix formation between the flake and spheroidal graphite cast irons. We discuss the influence of the sulfur and copper on the matrix in the flake and spheroidal graphite cast iron using the samples, which were melted in a 20kW alumina-lined 7kg high frequency induction furnace. We prepared them using electrolytic iron, electrode graphite, semi-conductor grade pure Si and pure Cu for obtaining a significantly low sulfur cast iron for the base samples. Chemical reagent FeS was used as the sulfur additive to the flake graphite samples. The melt was inoculated with 0.3% 75%Si-3%Ca ferrosilicon, and then cast into a shell mold of 30mm

inner diameter and 300mm length for observation of their microstructures.

The spheroidal graphite samples were prepared from the identical raw materials except for the FeS addition. The magnesium treatments were carried out with the addition of 2% ferrosilicon magnesium alloy, 45%Si-3.86%Mg-1.75%Ca-1.37%RE-1.03%Al, and after the spheroidal treatments, the melt was inoculated with 0.3% of 75%Si-3%Ca ferrosilicon, then cast into shell molds of 30mm inner diameter and 300mm length the observation for their microstructures. The target chemical composition of the parent metal was 3.7 % C-2.0%Si-0.01%Mn-0.005%P- 0.0024%S.

The chemical compositions of the experiment-1 samples are listed in Table 1 in which the notations of FC and FCD mean the flake and spheroidal graphite cast iron, respectively. All of these samples were cut and polished in order to observe their microstructures.

Table 1 Chemical composition of experiment-1 samples. (mass%)

TP No.	C	Si	Mn	P	S	Cu	Mg
FC-S free, Cu free	3.70	2.02	<0.01	0.0048	0.0022	0.0016	<0.0002
S free-0.5Cu	3.64	1.95	"	0.0043	0.0024	0.461	"
S free-1.0Cu	3.55	1.97	"	0.0045	0.0025	1.003	"
-0.01S-0.5Cu	3.66	1.99	"	0.0043	0.0083	0.529	"
-0.02S-0.5Cu	3.61	2.01	"	0.0047	0.0185	0.546	"
FCD-Cu free	3.78	2.04	"	0.0050	0.0026	0.0016	0.0424
-0.5Cu	3.93	2.00	"	0.0054	0.0030	0.477	0.0486
-1.0Cu	3.78	2.09	"	0.0050	0.0024	0.933	0.0463

In experiment-2, we studied the influence of the thermal history and copper on the ferrite and pearlite formation using flake graphite cast iron samples, comparing the as-cast samples to that of the heat treated ones. The cast iron melt was prepared as an commercial grade cast iron from a S25C bar, electrode graphite, metallic Si and pure Cu. The chemical composition of the S25C bar was as follows:

0.27%C-0.21%Si-0.46%Mn-0.014%P-0.017%S.

The target chemical composition of the parent metal was 3.5 % C-2.4%Si-0.4%Mn-0.013%P-0.013%S and their copper contents were changed with the copper addition from 0.25% to 1.0%. The melting process was nearly identical to that of experiment-1 except for S25C. The chemical compositions of experiment-2 samples are listed in Table 2.

These melts were cast into two 30mm inner diameter and 300mm length molds and four CE cup molds for each melting. The CE cup mold had a 30mm inner diameter and 50mm length and was

equipped with a CA thermocouple at the center for obtaining the cooling curves; we labelled them the CE cup samples. The three CE cups were quenched in water during the eutectoid transformation and the fourth one was cooled in the mold to room temperature, these being the as-cast samples.

Table 2. Chemical composition of experiment-2 samples. (mass%)

TP No.	C	Si	Mn	P	S	Cu	Cr	Mo
0.25 Cu	3.59	2.42	0.41	0.013	0.013	0.25	0.039	0.015
0.5 Cu	3.37	2.41	0.40	0.013	0.012	0.49	0.039	0.015
1.0 Cu	3.48	2.42	0.41	0.013	0.013	0.95	0.039	0.015

These 300mm length bars were cut into 50mm length pieces and a 5mm diameter and 30mm depth hole drilled at the base center for the thermal analysis. These four samples, called HT samples, were heated to 850°C or 950°C for 1h and cooled from these temperatures in air, then the three samples were quenched, while the fourth one was cooled to room temperature identical to that of experiment-1.

### 3. Results and discussion

#### 3-1. Experiment-1

The influence of sulfur and copper on the matrix structure of the flake graphite cast iron is shown in Fig. 1. As can be clearly seen, if the sulfur content is more than 0.0083%, the matrix structure is fully pearlite, while, if the sulfur content is less than 0.0025%, the matrix structure is almost ferrite. Moreover, we did not recognize the copper effect on the pearlite formation in the flake graphite cast iron. As is well known, copper is a graphitizing element in cast iron. Nevertheless, we already reported that the effect of copper on the pearlite formation in spheroidal graphite cast iron can be explained by the formation of a copper thin film around the spheroidal graphite which prevents the diffusion of carbon to the graphite [7], then the matrix becomes fully pearlite.

If we consider the free sulfur content, which means the dissolved sulfur except for combined one such as MgS and MnS, the free sulfur content in the spheroidal graphite cast iron should be less than 0.0011% (or  $a_s = 0.008$ ) [8], or  $a_s = 0.002$  as Subramanian reported [9]. These values are much less than the 0.0025% in this experiment. These results show that the sulfur in the flake graphite iron is a very powerful pearlite stabilizing element, therefore, the bull's eye structure is very common in spheroidal graphite cast iron due to the ultra-low sulfur activity.

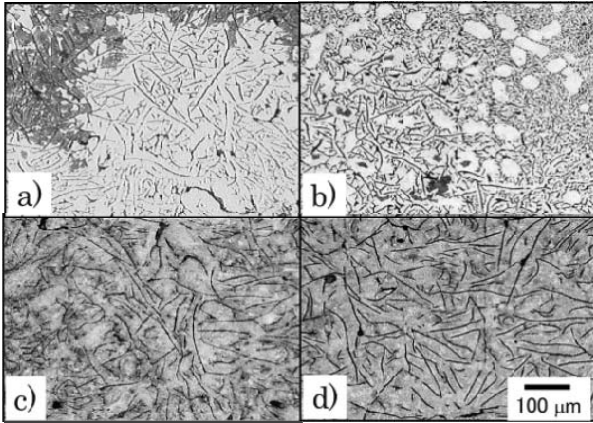


Fig. 1 Influence of S and Cu on matrix structure of as-cast flake graphite cast into 30mm samples. a) S & Cu free, b) S free-0.5Cu, c) 0.01S-0.5Cu, d) 0.02S-0.5Cu

Fig. 2 shows the influence of the graphite morphology and copper on the matrix structure for the S-free cast iron samples. As already mentioned, the copper in flake graphite cast iron is a ferrite stabilizing element, nevertheless, in the case of the spheroidal graphite cast iron, it is a very powerful pearlite stabilizing element as is well known. The copper in the flake graphite cast iron is a poor ferrite stabilizing element as shown in Figs. 1 and 2.

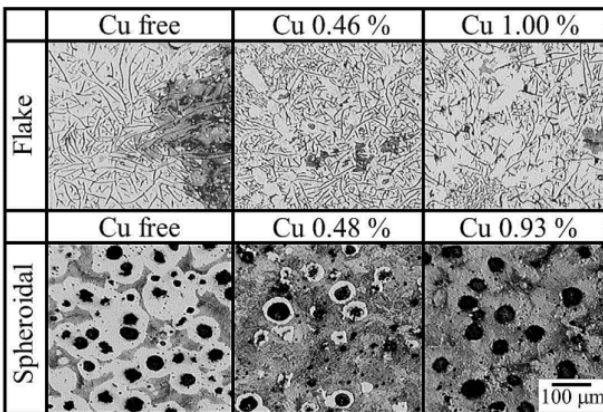


Fig. 2 Influence of graphite morphology and Cu on matrix structure for S-free 30mm samples.

### 3-2. Experiment-2

The graphite morphology and matrix structure of the as-cast flake graphite samples are shown in Fig. 3. These results are identical to that of Figs. 1 and 2, namely, the copper does not affect the graphite morphology and the matrix structure. The matrix of all the samples is pearlite due to the 0.013%S content as already mentioned. These results show that the pearlite stabilizing sulfur effect in the flake graphite cast iron is much stronger than the ferrite stabilizing effect of copper.

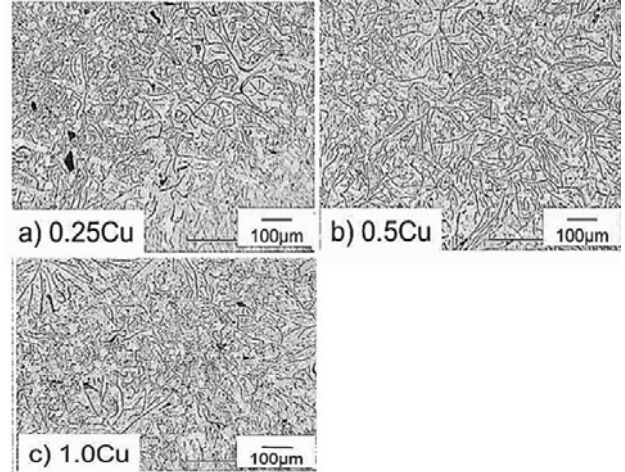


Fig. 3 Graphite structure of the as-cast 30mm samples. (0.013%S, full pearlite matrix).

Cooling curves, the differential curves,  $dT/dt$ , and the quenching temperature for the 0.25Cu CE cup samples are shown in Fig. 4. As can be clearly seen, the quenching interval was nearly periodic from ①-sample to ③-sample, and ④-sample was cooled in the CE cup to room temperature, thus, the cooling condition was identical to that of the 30mm bar as the cast sample and the matrix structure is fully pearlite as already described. Moreover, we can recognize the recalescence, in these figures, which should be the pearlite formation and these details will be discussed later.

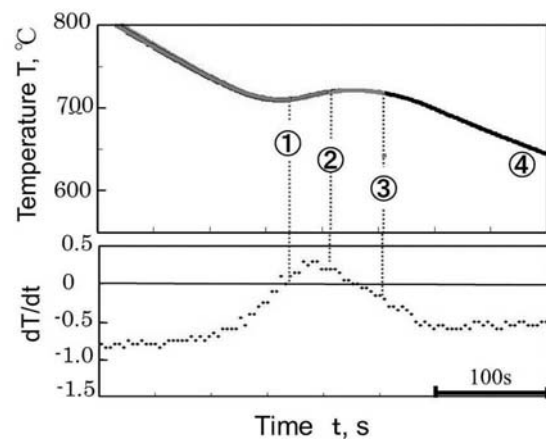


Fig. 4 Cooling curves, the differential curves during eutectoid transformation and quenching temperature of 0.25Cu CE cup samples, cooled from melts.

The microstructures of the ① to ④ samples are shown in Fig. 5. The microstructure of the ①-sample is the mixture of troostite and austenite, that of the ② is a small amount of pearlite in austenite, ③ is nearly a pearlite structure and a small amount of austenite, and that of ④ is fully pearlite as already mentioned.

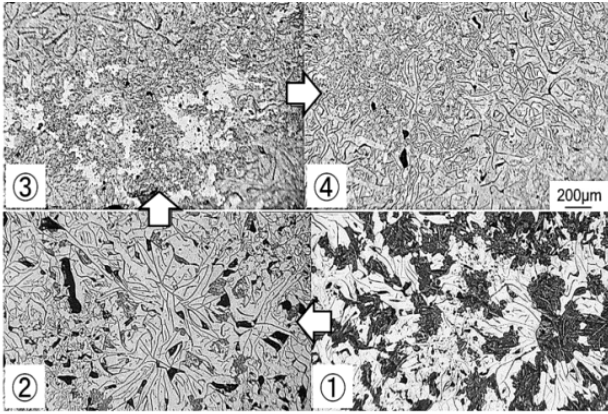


Fig. 5 Matrix structure of quenched 0.25Cu samples at different temperatures cooled from melts.

Four cooling curves of the 0.25Cu HT samples, cooled from 950°C, are shown in Fig. 6. Compared to Fig. 4, there is no clear recalescence in these cooling curves because the  $dT/dt$  values remain nearly zero at the onset of the eutectoid transformation. The influence of the thermal history on the cooling curves of the 0.25Cu HT samples, are shown in Fig. 7. The a) curve is the cooling curve of the CE cup, b) is that of the HT sample cooled from 950°C and c) is that of the HT sample cooled from 850°C. The CE cup sample was cooled in the mold, but the HT samples were cooled without a mold, then the cooling rate of the HT samples was higher than that of the CE cup sample. The distinct recalescence in these cooling curves is recognized only in the CE cup sample, nevertheless, in the HT sample's ones, there is no recalescence.

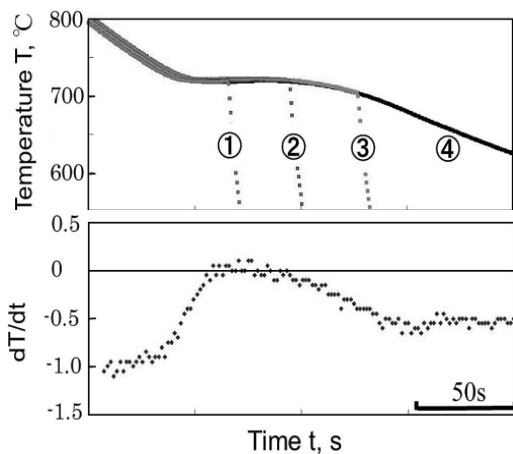


Fig. 6 Cooling curves, the differential curves and quenching temperature of 0.25Cu HT samples cooled from 950°C.

Fig. 8 shows the microstructure of these ④ samples. As can be seen clearly, that of the a) sample is fully pearlite, nevertheless, in the b) and c) samples, there are small amounts of ferrite around the A-type flake graphite. To confirm the influence of the thermal history on the pearlite fractions, we summarize all the data in Table 3. As clearly seen, we cannot find any pearlite formation effect by copper, however, the thermal history significantly affects the pearlite fraction. The matrix of these as-cast ones is fully pearlite, however, the pearlite fractions of the samples cooled from 950°C and 850°C are 60 to 70% and 39 to 47%, respectively. Why the thermal history is so significantly affected?

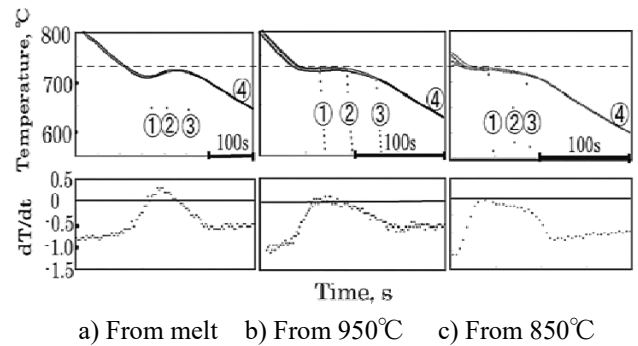


Fig. 7 Influence of thermal history on cooling curves of 0.25Cu CE and HT samples.

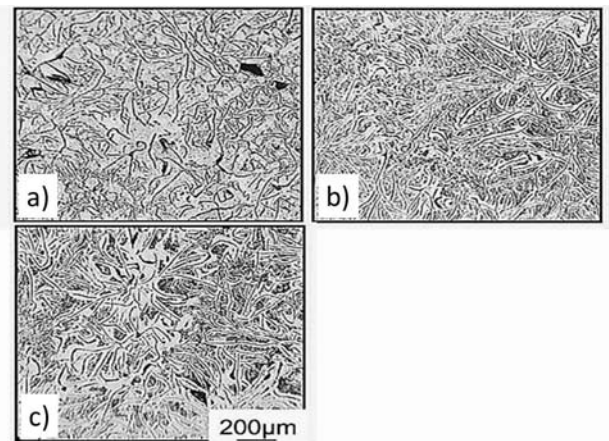


Fig. 8 Influence of holding temperature on matrix structure for air cooled 0.25Cu ④ samples in Fig. 7.

Table 3 Influence of thermal history and Cu content on pearlite fractions in flake graphite cast iron.

TP No.	As cast	Cooled from 950°C	Cooled from 850°C
0.25Cu	100%	65%	39%
0.5 Cu	100%	60%	41%
1.0 Cu	100%	70%	47%

Suppose that the solubility of carbon in the austenite can be estimated from the Fe-C-2.4%Si phase diagram with the function of the heating temperature as shown in Fig. 9. In this figure, we assumed that the heating temperature of the CE cup sample is 1150°C, thus the solubility becomes 1.6%, while that of the HT sample heated at 950°C is 1.0% and that of the 850°C sample is 0.7% as shown in this figure. We can then confirm that the solubility limit is the main factor which affects the ferrite and pearlite transformation in the cast iron.

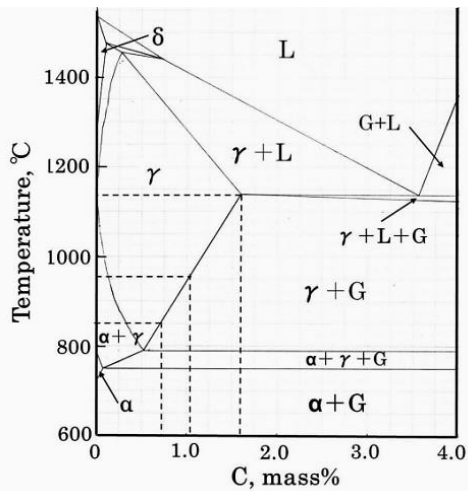


Fig. 9 Influence of heating temperature on solubility of carbon in austenite by the Fe-C-2.4%Si phase diagram

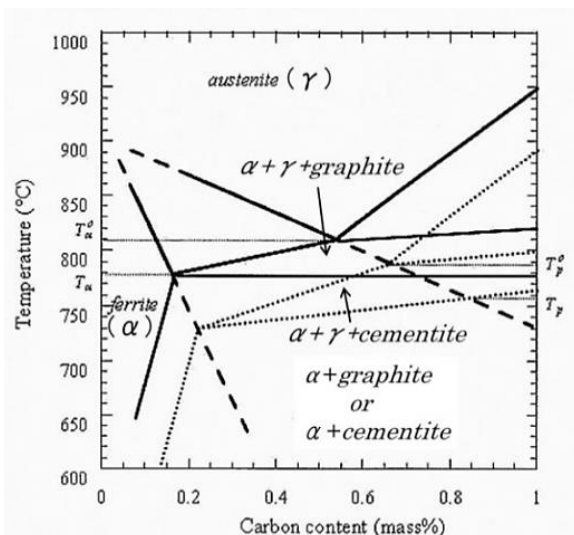


Fig. 10 Isoleth section of Fe-C-2.5%Si phase diagram reported by Gerval

For the discussion of the relationship between the cooling curves and the matrix structure, we have to use the stable and unstable eutectoid transformation diagram of cast iron [10,11], then we quoted

Gerval's diagram, shown in Fig. 10 [10]. There are two eutectoid transformation regions, namely, a ferrite transformation area located above the pearlite transformation area. The transformations in Figs. 7 b) and c) commence at the ferrite formation followed by the pearlite formation. Nevertheless, we could not find any clear recalescence in these figures, but there is a clear recalescence in Fig. 7 a), namely the pearlite transformation as already shown in Fig. 8.

### 3-3. Influence of graphite morphology on matrix structure

The ferrite formation frequently occurs in the D-type graphite area and in dendrites as is well known shown in Fig. 11. These phenomena can be mainly explained by the diffusion distance of carbon from the austenite to the graphite. Namely, if the diffusion distance is short, such as in the D-type graphite area, the carbon in the austenite can easily diffuse to form the ferrite as show in Fig. 12. Under this condition, if the carbon content in the austenite is low, it easily transforms into ferrite, thus this is the main reason for the thermal hysteresis.

However, the pearlite occurs at the eutectic cell boundary due to the micro-segregation of manganese and silicon in the matrix [5,7].

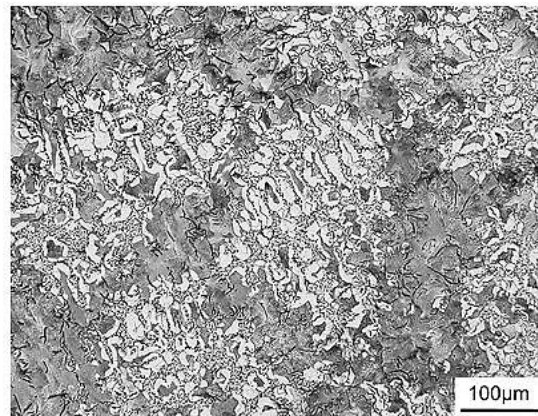


Fig. 11 Ferrite formation in D-type graphite area and dendrite area.

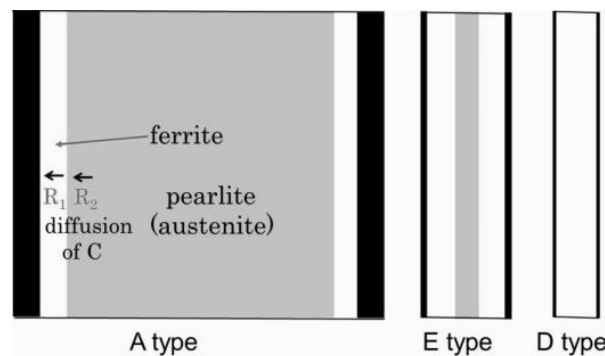


Fig. 12 Influence of graphite morphology on ferrite formation in flake graphite cast iron.

There is a significant difference in the ferrite formation mechanism between the flake and spheroidal graphite cast irons in the diffusion field, namely, rectangular coordinate diffusion in the flake graphite iron and spherical coordinate diffusion in the spheroidal graphite iron. This mechanism can be illustrated in Fig. 13. Therefore, if the cooling rate is high, such as a normalizing treatment, the pearlite structure can easily occur due to the spherical coordinate diffusion.

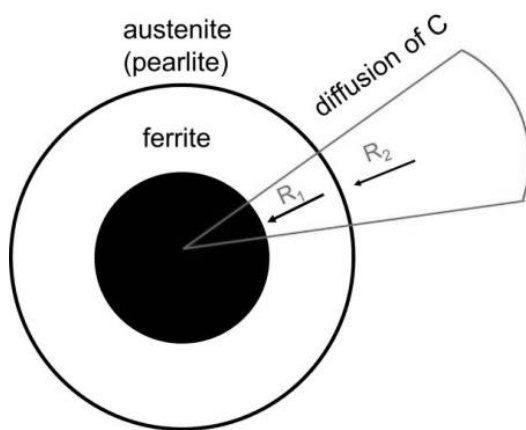


Fig. 13 Ferrite formation mechanism in spheroidal graphite cast iron.

The pearlite formation effect of Sn and Sb is due to the adsorption of these elements at graphite/matrix interface, as already reported by Johnson et al [12]. Nevertheless, the effect of Cu is limited only to spheroidal graphite cast iron as already mentioned [7].

#### 4. Conclusions

We discussed the influence of the graphite morphology, thermal hysteresis, and sulfur and copper contents on the ferrite/pearlite transformation in cast iron based on microstructure observations and their cooling curves. In this study, a number of experiments were conducted using the flake and spheroidal graphite cast irons. The conclusions are as follows:

1. The sulfur in the flake graphite cast iron is a powerful alloying element for the pearlite formation.
2. The copper is a pearlite stabilizing element in the spheroidal graphite cast iron, however, it is a ferrite stabilizing element in the flake graphite cast iron.
3. The heating temperature during the heat treatment affects the carbon solubility in the austenite, and the temperature affects the ferrite/pearlite transformation. A low heating temperature produces more ferrite structure than that at a high

temperature, then the fully pearlite structure can be formed in the as-cast samples.

4. A recalcrescence is observed during the pearlite transformation, but no significant recalcrescence can be observed in the ferrite/pearlite samples.
5. The ferrite and pearlite transformations are controlled by the sulfur content, the carbon diffusion distance and the field.

#### References

- [1] G. Ohira and K. Ikawa: AFS Trans. 66(1958)526
- [2] J. Lacaze, C. Wilson and C. Bak: Scandinavian J. Metallurgy 23(1994)151
- [3] T. Skaland, Ø. Grong and T. Grong: Metallurgical Trans. A: 24A(1993)2347
- [4] T. Szykowny and M. Trepzyńska: Archives of Foundry Eng. 10(2010,3)101
- [5] R.-B. Zao, S. Ueno, S. Yamada, K. Sugita and H. Nakae: Intern's J. Cast Metals Res. 21(2008)62
- [6] H. Nakae, K. Sigita and B.-R. Zhao: J. JFS 78(2006)457
- [7] Y. Zou, K. Komada and H. Nakae: J. JFS 83(2011)378
- [8] S. Jung, T. Ishikawa and H. Nakae: Materials Sci. and Eng. A 476(2008)350
- [9] S. V. Subramanian, D. A. R. Kayn and G. R. Purdy: Mater. Res. Soc. Symp. Proc., 34(1985)47
- [10] V. Gerval and J. Lacaze: ISIJ International 40(2000)386
- [11] P. Mrvar, M. Petrič and J. Medved: Key Eng. Mater. 457(2011)163
- [12] W.C. Johnson and B.V. Kovacs: Metallurgical Transaction A 9A(1978)219